FINAL TECHNICAL REPORT

NEHRP/USGS AWARD NUMBER G09AP00009

Simulation of Fault System Seismicity: Applications to Probabilistic Assessments of Earthquake Occurrence

Principal Investigator: James Dieterich
University of California, Riverside
Department of Earth Sciences
454 Geology Building
Riverside, CA 92521

Tel: 951-827-2976

Fax: 951-827-2976

Email: dieterichj@ucr.edu

Term Covered by award: January, 2009 – December 2010

ABSTRACT

Current standard methodologies for assessing earthquake probabilities are based on models of regional seismicity that employ generic probability distributions for earthquake occurrence and simplified approximations of the physical processes, constitutive properties, and interactions that control the onset of and extent of earthquake slip. A promising avenue for improving assessment methods, and reducing the large uncertainties in current assessments, is to incorporate more accurate, and region-specific, characterizations of the interactions and physical processes that control earthquake occurrence in fault systems. This project has carried out large-scale simulations of earthquake occurrence to characterize system level response of fault systems including processes that control time, place and extent of earthquake slip. The simulation method incorporates both earthquake and fault creep processes. Simulations have been used to investigate the relationships between fault geometry and earthquake occurrence, stress interactions, the relationships between catalog statistics and physical parameters in the model, earthquake clustering, and repeating earthquakes where fault creep and earthquake slip are coupled. Various avenues for using earthquake simulators in probabilistic assessments of earthquake probabilities were investigated. These include use of the model to generate site-specific probability density functions for earthquake occurrence across a range magnitudes and characterization of clusters of large events.

Background

The physical processes governing the occurrence of earthquakes in fault systems are undoubtedly complex, varied, and poorly understood. The current inadequate state of knowledge severely limits our predictive abilities to extrapolate empirical characterizations of seismicity to conditions where observations are sparse (including large earthquake magnitudes, short observation intervals, and possible variability between narrowly defined geographic regions). And it restricts interpretations of seismological observations in terms of material parameters and physical conditions. This project focuses on the behavior of fault systems particularly the physical parameters, processes, and interactions that control the space/time characteristics of earthquakes. In addition to its use as a tool to investigate fundamental topics in earthquake physics, fault system simulations can provide new avenues for improving the regional evaluations of earthquake probabilities, which are an important activity of the USGS earthquake hazards program.

The recently completed assessment by the 2007 Working Group on California Earthquake Probabilities is an impressive and valuable achievement. However, like previous probabilistic assessments, it is based on *ad hoc* and complicated models of regional seismicity that employs generic probability distributions for earthquake occurrence, and approximations of the physical processes, constitutive properties, and interactions that control the onset of and extent of earthquake slip. The 2007 assessment employs a long list of assigned parameters that are poorly defined and must be set by expert opinion. Epistemic uncertainty (model uncertainty) is the primary reason for the complexity of probabilistic assessments of earthquake occurrence, and it is a major source of the large uncertainties in those assessments. In conjunction with the 2007 Working Group on California Earthquake Probabilities a workshop was held in March 2007, at Lake Arrowhead, California, to discuss approaches and issues relating to time-dependent assessments. A listing of major issues and questions raised at the workshop included 1) failures of competing idealized probability models (Poisson, clustered, quasi-periodic) to fully represent the range of characteristics in earthquake catalogs; 2) uncertainty in assignment of parameter values for the probability density functions; 3) uncertainty concerning both the validity and implementation of the characteristic earthquake and fault segmentation models; 4) lack of specific criteria for setting segment boundaries and for establishing probabilities for multi-segment rupture events, 5) uncertainty in how to parameterize and implement the possibility of fault-to-fault jumps and rupture branching; 6) intrinsic problems with idealized models (such as time-predictable, slip-predictable, and slip deficits) that do not properly capture the relationships between stress and slip in 3D systems; 7) ambiguities in quantifying the effects of fault stress interactions, which are spatially variable, to determine an overall clock change parameter for computing time-dependent probabilities; and 8) uncertainty in the quantification of event-to-event variability of stress changes or slip of rupture processes. To address many, if not most, of these issues will require physics-based modeling of earthquakes in fault systems.

Faults in nature are geometrically complex – they exhibit roughness at all length scales

[Scholz and Aviles, 1986; Power and Tullis, 1991; Sagy and others, 2007] and form branching structures and networks. A number of studies have examined various aspects of fault geometry on fault slip and earthquake processes. Some examples include investigation of slip of wavy faults [Saucier and others, 1992; Chester and Chester, 2000], slip through idealized fault bends [Nielsen and Knopoff, 1998], rupture propagation into fault branches [Oglesby and others, 2003; Fliss and others, 2005] and rupture jumps across gaps [Harris and others, 1991; Duan and Oglesby, 2006]. Simulations of regional fault-system seismicity [Ward, 1996, 2000; Rundle and others, 2004] demonstrate that integrative models of regional earthquake activity in fault systems can be developed that broadly satisfy historic and paleoseismic data. This project builds on those efforts by developing an accurate and more comprehensive computational model for fault slip and earthquake occurrence in geometrically complex fault systems. The model incorporates the following features.

- High-resolution representations of complex fault system geometry. In the current single-processor code, up to 30,000 fault elements can be represented with strike-slip, dip-slip, and mixed-mode faulting.
- A very efficient computational approach together with high resolution modeling of fault systems, that permit simulation of large numbers of earthquakes ($>10^5$) in the range M4.0 – M8.0 (using 1km^2 fault elements). This enables effective exploration of parameter space and comparisons with earthquake catalog data.
- Use of rate- and state-dependent fault constitutive properties for simulation of time-dependent earthquake nucleation processes, which results in spatial and temporal clustering of earthquakes including foreshocks and aftershocks.
- Quasi-dynamic rupture propagation and dynamic triggering.
- Calibration and validation against fully dynamic FEM simulations.

Modeling approach

The wide range of length scales to be modeled, and the need to repeatedly simulate long earthquake catalogs to investigate effects of parameters and processes on seismicity, point to the importance of computational efficiency for this effort. Clearly, it is not feasible with current technology to attempt repeated simulations of synthetic catalogs of $>10^5$ earthquakes using a detailed fully dynamical deterministic calculation of each earthquake. Appropriate large-scale approximations and simplifications must be developed that provide acceptably accurate solutions while allowing the computations to be done in a reasonable time. For this project we have implemented a highly efficient computational approach developed and tested by Dieterich [1995]. Ziv [2003] and Ziv and Rubin [2003] used some elements of this method to study clustering processes and frequency statistics. Tests described below indicate the calculations are quite accurate.

The computer code is based on a boundary element formulation whereby interactions among the fault elements are represented by an array of 3D elastic dislocations, and Coulomb stress on the elements in the direction of slip on an element is

$$S_i = K_{ij}\delta_j + S_{L_i} \quad , \quad i,j = 1,2,...,n \qquad (1)$$

where K_{ij} is an interaction matrix derived from the elastic dislocation solutions, δ_j is slip

of fault element j, S_{t_i} is the externally applied (tectonic) stressing at fault element i, and n is the total number of elements (summation convention applies to repeated indices). The code uses the full 3D boundary element representations and it can employ rectangular or triangular fault elements. The model employs rate-state constitutive properties [Dieterich, 1979, 1981; Ruina,1983; Rice, 1983] with full coupling of normal stress to fault strength through the coefficient of friction and the friction state-variable θ , which evolves with time, slip and changes of normal stress as given by Linker and Dieterich [1992]. The central feature of the method is the use of event-driven computational steps as opposed to time stepping at closely spaced intervals. The cycle of stress accumulation and earthquake slip at each fault segment is separated into three distinct phases designated as sliding states 0, 1, and 2. A fault element is at state 0 if stress is below the steady-state friction, as defined by rate- and state-dependent friction. In the model this condition is approximated as a fully locked element in which the fault strengthens as the frictional state variable θ increases with time, *e.g.* $\theta = \theta_0 + t$ at constant normal stress, but modified by effects arising from normal stress changes. The transition to sliding state 1 occurs when the stress exceeds the steady-state friction. During state 1, conditions have not yet been met for unstable slip, but the fault progressively weakens. Macroscopic slip is negligible. Analytic solutions for nucleation of unstable slip [Dieterich, 1992] generalized for varying normal stress [Dieterich, 2007; Richards-Dinger and Dieterich, in preparation], together with stressing rate determine the transition time to state 2, which is earthquake slip. At tectonic stressing rates earthquake nucleation typically requires a year or more, but during earthquake slip the high stressing rates at the rupture front compress the duration of state 1 to a fraction of a second.

During earthquake slip, the simulation method employs a quasi-dynamical representation that approximates the gross dynamics of the earthquake source. Slip speed during an earthquake (state 2) is set at a constant value using the relationship for elastic shear impedance together with the local dynamic driving stress

$$\dot{\delta}_{EQ_j} = \frac{2\beta\Delta\tau_j}{G} \quad , \qquad (2)$$

where the driving stress $\Delta\tau_j$ is the difference between the stress at the initiation of slip and the sliding friction at element j, β is the shear wave speed, and G is the elastic shear modulus. The use of (2) provides a quasi-dynamical representation of time-scales and slip rates for the earthquake event simulations. Some characteristics of the rupture dynamics, and comparisons of single-event rupture simulations with fully dynamical simulations in 3D are discussed below. An element ceases to slip and reverts to state 0 when the stress decreases to some specified stress determined by the sliding friction (with inertial overshoot of stress to levels less than the sliding friction as an adjustable model parameter). Computational efficiency is obtained from the use of event-driven computational steps, use of analytic nucleation solutions, and specification of earthquake slip speed from the shear impedance relation. Note that change of stressing rate at any element i in response to initiation or termination of earthquake slip at element j is simply

$$\Delta\dot{S}_i = \pm K_{ij}\dot{\delta}_{EQ_j}. \qquad (3)$$

Hence, 1→2 or 2→0 state transition events require only one multiply and add operation at each element to update stressing rates everywhere in the model (no system-scale updates are required for the 0→1 transition). Because the transition times depend only on initial conditions and stressing rates, computations proceed in steps that mark the transition from one sliding state to the next without calculation of intermediate steps. This approach completely avoids computationally intensive solutions of systems of equations at closely spaced time intervals. Computation time for an earthquake event of some fixed size, embedded in a model with n fault elements, scales approximately by n^1.

During the period covered by this report the RSQSim code was was modified to include continuously creeping fault elements. This is modeled with rate- and state-dependent fault friction

$$\mu = \mu_0 + a\ln(\dot{\delta}) + b\ln(\theta) \qquad (4)$$

where the parameters a and b are set to give rate-strengthening slip assuming steady-state frictional response. With this addition, large earthquake ruptures can penetrate into a deep creeping zone and large earthquakes are characteristically followed by an interval of afterslip, which drives time-dependent post-seismic deformation and stressing. Figure 1 illustrates examples of a M7.4 and M6.2 earthquake from a 200,000 event simulation with a simple planar fault.

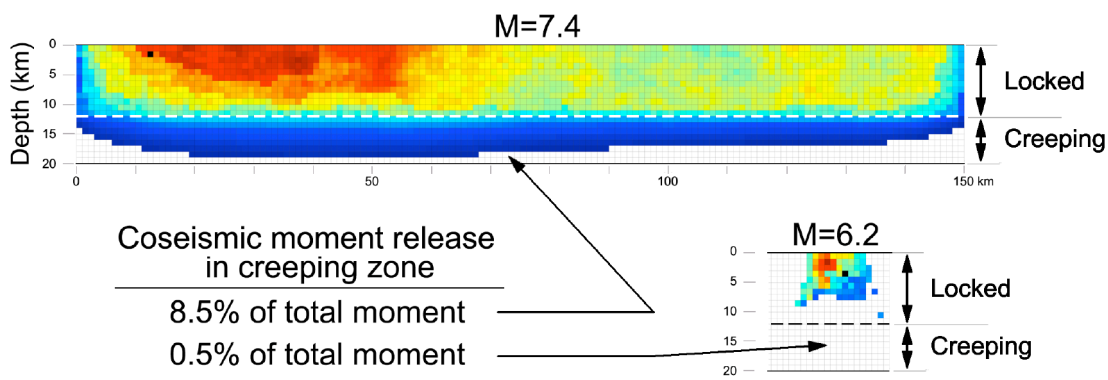

Figure 1. Rupture simulations with a zone of fault creep at the base of the fault. Red indicates maximum slip. Constitutive parameter are a=0.010, b=0.015 in the locked (seismogenic) zone and a=0.010, b=0.008 in the creeping zone.

Results

During the report period the RSQSim code underwent several refinements and is now capable of routinely generating seismicity catalogs in fault system models with up to 30,000 elements. Models with about 5,000 fault elements take approximately 8 hours to simulate 500,000 events M4.6 to M8.0 on a single 2.5 GHz G5 CPU. We estimate that models with 30,000 fault elements and roughly 100,000 earthquakes (M4-M8) can be simulated in 12-24 hours. The computation speed of the code far outperforms that of any other method we know of, and will further improve with implementation of a parallelized version of the code that is now under development.

As a matter of good scientific practice we have endeavored to be rigorous in testing the simulator at every stage of development. A key performance measure of the rupture simulations is the accuracy with which the simulations predict a) the extent of earthquake rupture given a stress state at the initiation of an earthquake, and b) the slip distribution in that rupture, which determines the details of the stress state in the model following an earthquake (and therefore subsequent earthquake history). We have continued to validate the quasi-dynamic rupture aspects of our model via comparisons with results from the fully dynamic finite element code DYNA3D. Previous work (Burrill et al., 2007) has shown that on homogeneous planar faults the RSQSim results agree qualitatively and quantitatively very well with those of DYNA3D. In collaboration with David Oglesby of UC Riverside and a UCR undergraduate student, Jennifer Stevens, we have explored the properties of ruptures on variable strength planar faults. For this comparison, our asperity model consists of multiple rectangular zones of increased normal stress of varying size, location, and amplitude. In the comparison shown in Figure 2 one can see that these heterogeneities lead to much more complex patterns (both spatial and temporal) of rupture than in our previous comparisons. Ruptures slow upon entering a high normal stress barrier, wrap around the barriers, and produce brief bursts of supershear rupture speeds just beyond the barriers (Dunham et al., 2003). Both codes allow rupture propagation over significant zones of negative stress drop in these asperity regions. As with the previous, simpler comparisons (and using the same RSQSim model parameters) the rupture character, time evolution, and final stresses and slips agree remarkably well considering the quasi-dynamic approximations in RSQSim. The amplification of slip on the right side of the fault in the Dyna3D calculation relative to the RSQSim result may be an effect of dynamic waves, which are not yet represented RSQSim. Some of the differences between RSQSim and DYNA3D, as well as the fact that ruptures in RSQSim have more difficulty jumping discontinuous stepovers may due to the absence of dynamic stresses in RSQSim.

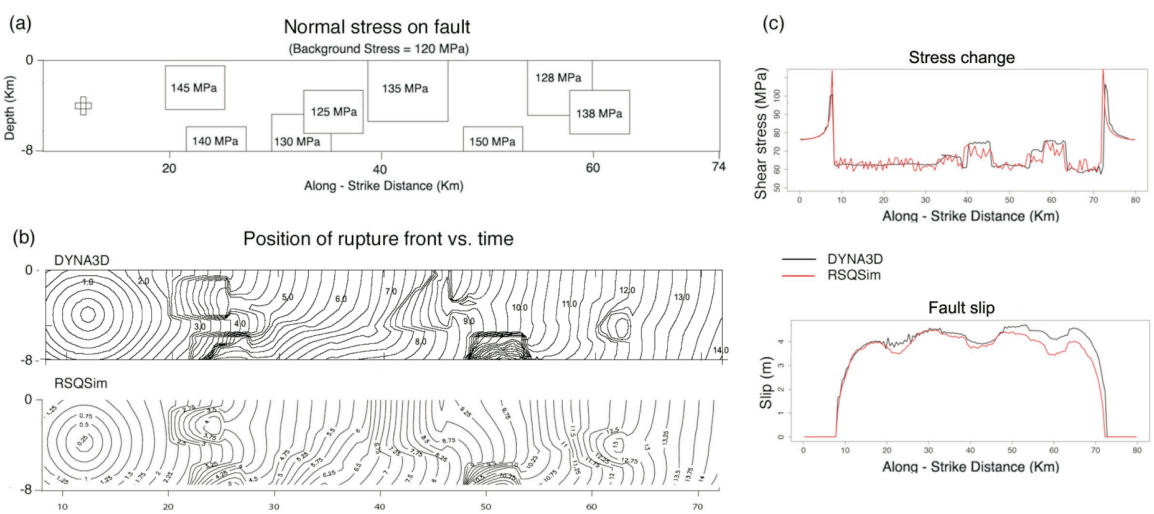

Figure 2. Comparison of rupture simulations with RSQSim and Dyna3D. (a) Normal stress distribution on fault surface. (b) Rupture initiation time (the contours map the rupture front as a function of time). (c) Stress change (left panel) and slip (right panel) along a profile at depth of 4.25 km. Fault elements for this simulation are 500mx500m.

We investigated the capability to implement dynamic stressing into the model. A promising approach, illustrated in Figure 3 is to use the quasi-dynamical simulations as a kinematic source to compute seismograms with the Greens functions for a homogenous elastic whole-space [*e.g.* Aki and Richards, 2002]. Because analytic solutions for earthquake nucleation can be used to determine if dynamic stresses trigger unstable slip (1→2 state transition) the implementation of dynamic triggering of slip should not be too costly in terms of computational speed. In current comparisons, the RSQSim seismograms from ruptures in models with homogeneous initial stress are approximately a factor of 2 smaller than those in DYNA3D due to our use of whole-space Greens functions. The addition of image source Greens functions should bring the solutions to with about 10-15% of DYNA3D. Complex ruptures with heterogeneous initial stresses inherited from previous events in a long simulation in RSQSim produce realistic seismograms.

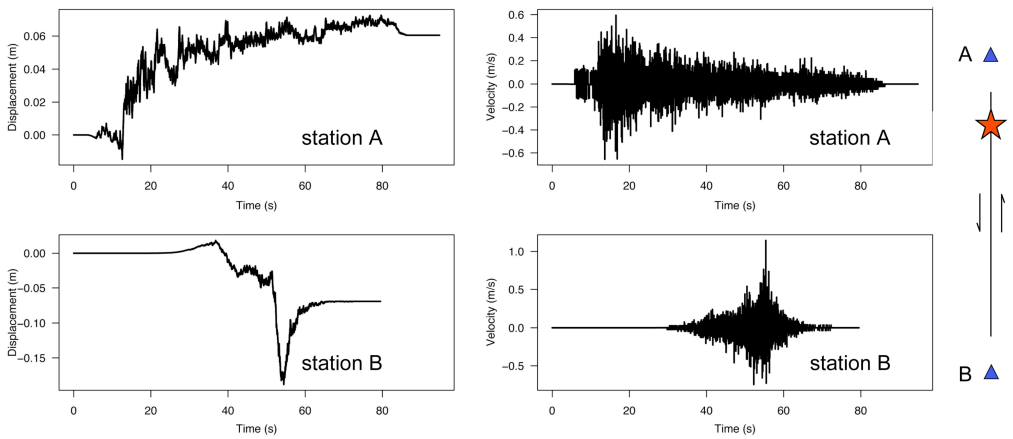

Figure 3. Displacement (left) and velocity (right) seismograms at stations A and B, produced by a complex rupture with heterogeneous initial stresses from a simulation with 50,000 events. Rupture is unilateral starting at the location of the star.

Figure 4 illustrates an implementation of fault creep in RSQSim to model regularly repeating earthquakes, which are represented as small seismogenic patches (a<*b*) surrounded by fault elements that undergo continuous stable fault creep. In the simulations the small repeating earthquakes occur at regular intervals of 3 to 10 years, depending on location, until a large earthquake (M~6.5) occurs on the large seismogenic patch (right half of model in Figure 4). Following large earthquakes, afterslip on the creeping sections of the fault increases with the logarithm of time. This transient increase of creep rate greatly shortens the recurrence interval of the small repeaters. The rate of occurrence of the repeaters then decays by 1/t in agreement with the Omori aftershock decay law (Figure 4b). Identical behavior of repeaters was observed by Schaff and others (1998) following the 1989 Loma Prieta earthquake (Figure 4c).

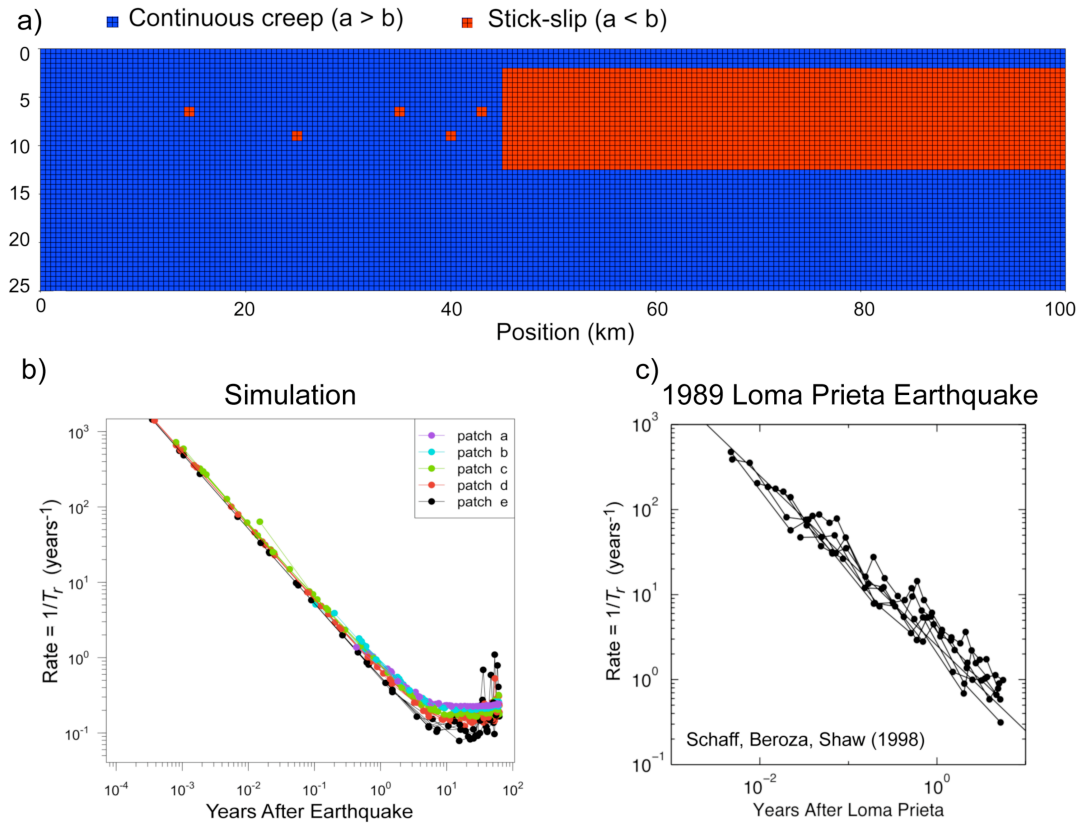

Figure 4. Simulation of repeating earthquakes. a) Model of fault with seismogenic patches (red) embedded in creeping fault (blue). The small seismogenic patches on the left side of the model produce highly regular repeating events. b) Earthquake rates following large events on the large seismogenic section of the fault (right), showing 1/t decay. c) An idential response of repeaters was observed by Schaff and other (1998) following the 1989 Loma Prieta earthquake.

Our principal research effort focused on the statistics of earthquake recurrence for use in probabilistic estimates of future damaging earthquakes. As noted above, current methods for estimating earthquake probabilities, conditional on elapsed time since the previous event, are based on idealized probability density distributions that have a limited basis in observations because the instrumental record is so short compared to typical earthquake recurrence times. In this study we employed RSQSim to produce long earthquake catalogs to generate empirical density distributions at a specific location. The results of this investigation are presented in the paper Dieterich and Richards-Dinger (2010). Highlights of that study are summarized here.

At the most general level, the statistics of earthquake occurrence are determined by the system-level dynamics of fault slip interactions. Probability density distributions for recurrence of earthquakes above some threshold magnitude M_{min}, at some location on a fault, are of primary interest for time-dependent probabilistic estimations. We find that fault system geometry is a strong determinant of system interactions. Simulations show that the probability density distributions of recurrence times for slip of isolated faults

(planar, fractally rough, or fractally segmented) change with M_{min} and form a narrow characteristic earthquake peak at high magnitudes. The characteristic earthquake peak occurs because earthquake ruptures that reach a critical size (about 10 km for faults that extend from the surface to a depth of 15 km) have a strong tendency to continue to propagate to the limits of the model. The resulting end-to-end ruptures are highly periodic because the stress after the earthquakes is reset to a similar average state following each end-to-end rupture. Strong fractal segmentation of faults reduces the periodicity and in the extreme eliminates end-to-end ruptures.

In contrast to the relatively simple recurrence distributions seen for isolated faults, the distributions for fault sections within fault systems (see Figure 5) are more complex and variable. The distributions take a variety forms that change with position within the fault system. In addition, the recurrence intervals have much wider distributions than isolated faults. None of the distributions in Figure 5 can be fit with any of the standard analytic probability density functions (PDFs) used to model earthquake recurrence times (e.g. lognormal, Weibull, Brownian passage time). However, in some cases the distributions can be approximated by a combination of a power-law and one of the aforementioned quasi-periodic distributions. Significantly, the distributions appear to be controlled by large-scale system geometry, and are rather insensitive to local details such as the addition of fault roughness. Limited tests that vary element dimensions and use different combinations of constitutive parameters show that the results are quite stable. These characteristics indicate that gross fault system geometry plays a primary role in establishing the characteristics of stress evolution that control earthquake recurrence. Above some limiting separation, fault stepovers form effective impediments to the propagation of earthquake ruptures and have a significant though lesser impact on the recurrence distributions.

In the context of procedures for estimating long-term probabilities of earthquakes, the simulation results indicate the following. A) epistemic uncertainty relating to choice of recurrence models appears to be significantly greater than that represented by the range of commonly used quasi-periodic distributions. B) The shapes of the distributions depend strongly on earthquake magnitude and position within a fault system. Currently these factors are not considered in estimates of earthquake probabilities. C) The strong control of the of density distributions by fault system geometry, which is observable, indicates that use of simulation-generated distributions can greatly improve the accuracy and reliability probabilistic estimates.

In addition we find that earthquake nucleation with rate- and state-dependent friction strongly affects the statistics of earthquake recurrence in the simulations, particularly at short time intervals and at smaller earthquake magnitudes. Density distributions of recurrence intervals have very narrow peaks at the shortest times (~years) that consist of foreshocks, aftershocks, and earthquake clusters. See, for example, the extremely steep slopes near the origin in the cumulative distributions in Figure 5. Rates of recurrence within this peak follow Omori's Law and decay by $t^{-0.8}$. Clustering in the form of large-earthquake pairs (and more rarely triples) is a consistent feature of the fault system simulations, but at somewhat low rates (20% of $M \geq 7$ events are followed within 4 years

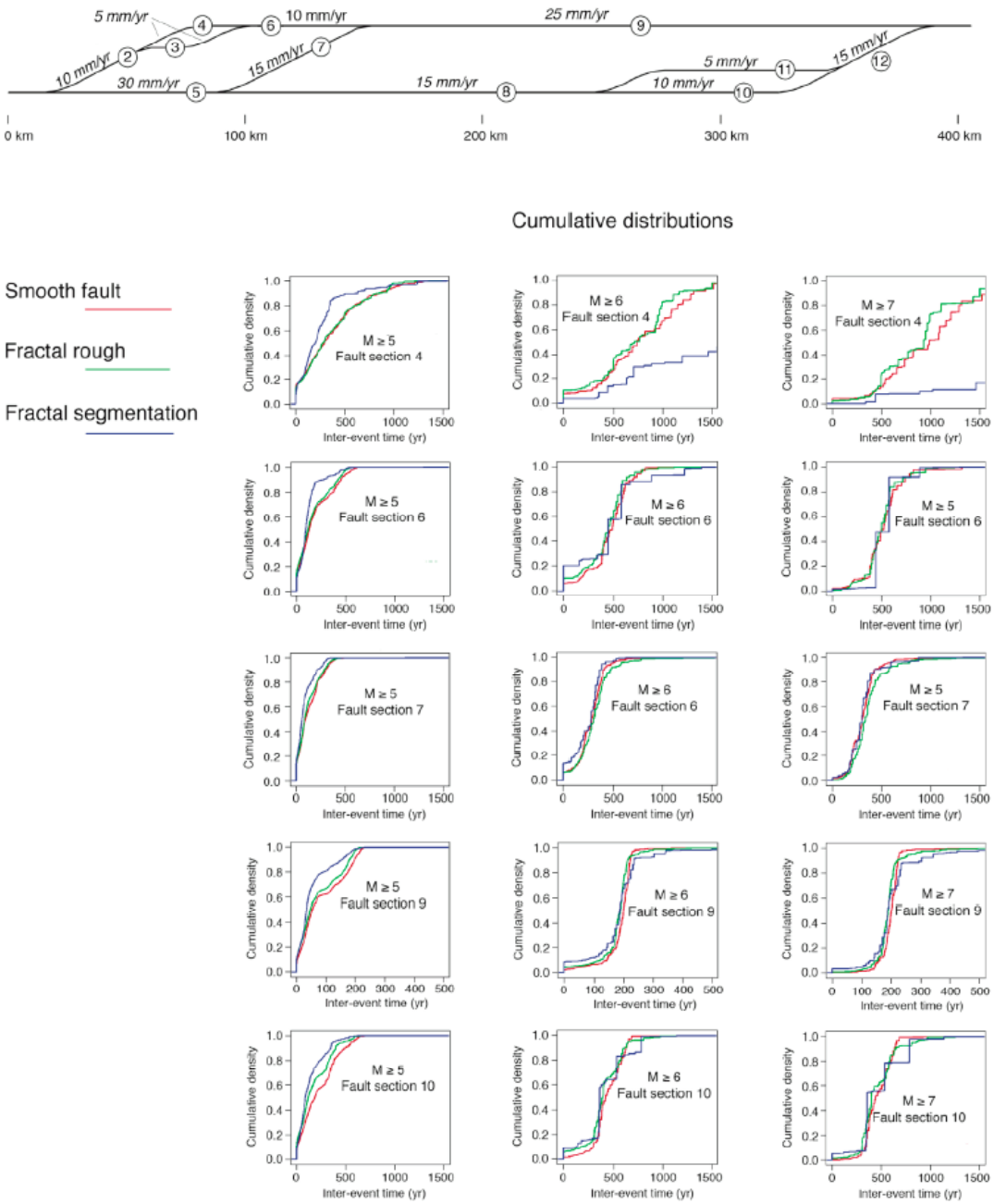

Figure 5. Cumulative probability distributions of recurrence times for earthquakes of various magnitudes on selected sections of an idealized fault system (upper panel) with three different forms of small-scale geometry: smooth fault sections (red), fractal roughness with $\beta = 0.1$ (green), and fractal segmentation with $\beta = 0.04$ (blue). These are the distributions for waiting times between events larger than a given threshold to cause slip on the same point on the fault, stacked over all points on a given fault section (identified by the circled numbers in the upper panel). The parameter β controls the amplitude of the fractal roughness and segmentation.

by another such event, see Table 1). Intervals between large earthquake pairs vary from a few seconds to 4 years (our arbitrary cutoff to define large event clusters) and also follow an Omori decay, which is consistent with earthquake pairs in nature (Kagan and Jackson, 1991, 1999). From a regional earthquake hazard perspective the clusters represent a continuing interval of significantly increased hazard following large earthquakes. The follow-on events in large earthquake clusters initiate in the aftershock regions of the prior events and their occurrence correlates with especially high aftershock rates. There is little or no overlap of the areas of slip in the clusters.

Model	Total number of events	Number $M \geq 7$	Single events	Double events	Triple events
Planar faults	299,000	196	130	27.5	3.6
Fractal roughness $\beta = 0.1$	377,000	237	152	35.8	4.6
Fractal segmentation $\beta = 0.02$	394,000	221	144	36.1	1.8
Fractal segmentation $\beta = 0.04$	607,000	274	58.4	32.1	38.0

Table 1. Clustering of earthquakes $M \geq 7$ in fault system simulations. All numbers are per 10,000 years of simulated time.

Finally we note that with current standard methods, based on PDFs for earthquake recurrence intervals, the calculation of time-dependent probabilities using paleoseismic data and historical records of past earthquakes requires a number of interpretive and modeling steps that substantially increase uncertainties in ways that are difficult to quantify. Essentially, these interpretive steps convert very limited data on timing of an earthquake, and information on magnitude or amount of slip at a point on a fault, to a spatial distribution of slip over an assigned section of fault. Simulations provide the capability to define specialized empirical density distributions that directly utilize primary observational data without the interpretive steps and resulting uncertain assumptions of current methods. Figure 6 illustrates two examples of alternative distributions. The first distribution (Figure 6a) is defined in terms of magnitude of slip at an observation point in the prior earthquake. This distribution is that of the waiting time from the occurrence of slip exceeding some threshold at a given point until the next event that exceeds a given magnitude affects that same point. Distributions of this type directly can be employed to directly utilize paleoseismic data for amount of slip in the prior earthquake at some point on a fault to estimate probability of future earthquakes at that point. The second distribution (Figure 6b) is represents a case where the time and magnitude (with some uncertainty) of the prior earthquake are both known. The distribution gives information about both the time of the following event and also the likely magnitude. Both distributions relax the assumptions of characteristic earthquakes and allow for earthquakes of varying sizes. The results in Figure 6b are rather interesting. Broad quasi-periodic peaks for earthquakes M5 – M5.5 following a earthquake M5 – M5.5 are quite evident in these distributions, but the sub-distributions for $M \geq 7.5$ following M-5.5 earthquakes decay monotonically and roughly follow an exponential distribution indicating a constant Poisson rate of occurrence following a M5.5 event. Hence, is the occurrence of M=5.5 earthquake may have little predictive value for the the occurrence of $M \geq 7.5$ earthquakes. Some other examples of specialized density distributions that might be assembled directly from the synthetic catalogs include a)

situations where historical records indicate the prior earthquake may lie within a region but causative fault is uncertain, b) recurrence of slip exceeding some amount at a specific site, in some time interval (of possible interest for lifelines that cross faults), and c) probability of future earthquake by time and distance from a site.

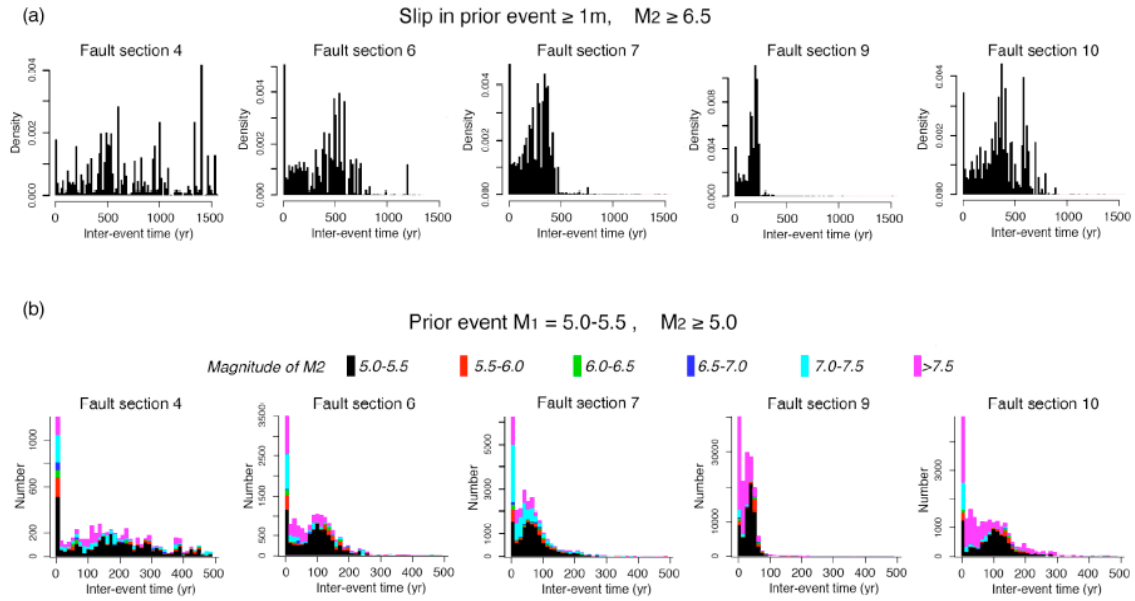

Figure 6. Examples of alternative parameterizations of density distributions of recurrence times. Data are from the smooth fault version the fault system model of Figure 5.

Publications

Dieterich, J. and K. Richards-Dinger, Earthquake recurrence in simulated fault systems, *Pure Appl. Geophys.*, 167, 1087-1104, 2010.

References

Aki, K., and P. G. Richards, Quantitative Seismology, 2nd Ed., University Science Books, 2002.

Burrill, C., K. Richards-Dinger, J. Dieterich, D.D. Oglesby, A Test of Two Earthquake Modeling Methods, Eos Trans. AGU, 88(52), Fall Meet. Suppl., Abstract S13D-08, 2007.

Chester, F. M., and J. S. Chester, Stress and deformation along wavy frictional faults, J. Geophys. Res., 105, 23,421– 23,430, 2000.

Dieterich, J. H., Modeling of rock friction 1. Experimental results and constitutive equations, J. Geophys. Res., 84, 2161–2168, 1979.

Dieterich, J., Constitutive properties of faults with simulated gouge, in Monograph 24, Mechanical Behavior of Crustal Rocks, edited by N. L. Carter, M. Friedman, J. M. Logan, and D. W. Sterns, pp. 103–120, American Geophysical Union, Washington, D.C., 1981.

Dieterich, J. H., Earthquake nucleation on faults with rate- and state-dependent strength,

Tectonophysics, 211, 115–134, 1992.
Dieterich, J. H., Earthquake simulations with time-dependent nucleation and long-range interactions, Journal of Nonlinear Processes in Geophysics, 2, 109–120, 1995.
Dieterich, J., Applications of rate-and-state-dependent friction to models of fault slip and earthquake occurrence, in Treatise On Geophysics, Vol. 4, edited by G. Schubert, Elsevier, Oxford, 2007.
Dieterich, J. and K. Richards-Dinger, Earthquake recurrence in simulated fault systems, PAGEOPH (in press), 2010.
Duan, B., and D. D. Oglesby, Heterogeneous fault stresses from previous earthquakes and the effect on dynamics of parallel strike-slip faults, J. Geophys. Res., 111, 5309–+, 2006.
Dunham, E., P. Favreau, and J.M. Carlson, A supershear transition mechanism for cracks, Science, 299, 1557-1559, 2003.
Fliss, S., H. S. Bhat, R. Dmowska, and J. R. Rice, Fault branching and rupture directivity, J. Geophys. Res., 110, 6312–, 2005.
Hardebeck, J. L., Stress triggering and earthquake probability estimates, J. Geophys. Res., 109, 4310–+, 2004.
Harris, R. A., R. J. Archuleta, and S. M. Day, Fault steps and the dynamic rupture process: 2-D numerical
simulations of a spontaneously propagating shear fracture, Geophys. Res. Lett., 18, 893–896, 1991.
Kagan, Y. Y., and D. D. Jackson, Long-term earthquake clustering, Geophys. J. Int., 104, 117–134, 1991.
Kagan Y.Y. and D.D. Jackson, Worldwide doublets of large shallow earthquakes. Bull Seismol Soc Am 89(5):1147–1155, 1999.
Linker, M. F., and J. H. Dieterich, Effects of variable normal stress on rock friction - Observations and constitutive equations, J. Geophys. Res., 97, 4923–4940, 1992.
Nielsen, S. B., and L. Knopoff, The equivalent strength of geometrical barriers to earthquakes, J. Geophys. Res., 103, 9953–9966, 1998.
Oglesby, D. D., S. M. Day, Y.-G. Li, and J. E. Vidale, The 1999 Hector Mine earthquake: The dynamics of a branched fault system, Bull. Seismol. Soc. Am., 93, 2459–2476, 2003.
Power, W. L., and T. E. Tullis, Euclidean and fractal models for the description of rock surface roughness, J. Geophys. Res., 96, 415–424, 1991.
Rice, J. R., Constitutive relations for fault slip and earthquake instabilities, Pure and Applied Geophysics, 121, 443–475, 1983.
Ruina, A., Slip instability and state variable friction laws, J. Geophys. Res., 88, 10,359–10,370, 1983.
Rundle, J. B., P. B. Rundle, A. Donnellan, and G. Fox, Gutenberg-Richter statistics in topologically realistic system level earthquake stress-evolution simulations, Earth, Planets, and Space, 56, 761–771, 2004.
Sagy, A., E. E. Brodsky, and G. J. Axen, Evolution of fault-surface roughness with slip, Geology, 35, 283, 2007.
Saucier, F., E. Humphreys, and R. I. Weldon, Stress near geometrically complex strike-slip faults – Application to the San Andreas fault at Cajon Pass, southern California, J. Geophys. Res., 97, 5081–5094, 1992.

Scholz, C. H., and C. A. Aviles, The fractal geometry of faults and faulting, in Earthquake Source Mechanics (Maurice Ewing Volume 6), edited by S. Das, J. Boatwright, and C. H. Scholz, pp. 147–155, American
Geophysical Union, Washington, D.C., 1986.
Ward, S. N., A synthetic seismicity model for southern California: Cycles, probabilities, and hazard, J. Geophys. Res., 101, 22,393–22,418, 1996.
Ward, S. N., San Francisco Bay Area earthquake simulations: A step toward a standard physical earthquake model, Bull. Seismol. Soc. Am., 90 , 370–386, 2000.
Working Group on California Earthquake Probabilities (WGCEP), Seismic hazards in southern California: Probable earthquakes, 1994-2024, Bull. Seismol. Soc. Am., 85 , 379–439, 1995.
Working Group on California Earthquake Probabilities (WGCEP) (2007), The Uniform California Earthquake Rupture Forecast, version 2 (UCERF 2). USGS Prof Pap 2007-1437, 2008.
Ziv, A., Foreshocks, aftershocks and remote triggering in quasi-static fault models, J. Geophys. Res., 108, 2498, 2003.
Ziv, A., and A. M. Rubin, Implications of rate-and-state friction for properties of aftershock sequence: Quasi-static inherently discrete simulations, J. Geophys. Res., 108 , 2051, 2003.